ACS APPLIED MATERIALS & INTERFACES

Research Article

www.acsami.org

Controlled Fabrication of Microparticles with Complex 3D Geometries by Tunable Interfacial Deformation of Confined Polymeric Fluids in 2D Micromolds

Chang-Hyung Choi,[†,§,∥] Byungjin Lee,[†,∥] Jongmin Kim,[†] Jin-Oh Nam,[†] Hyunmin Yi,[‡] and Chang-Soo Lee*[,†]

[†]Department of Chemical Engineering, Chungnam National University, Yuseong-gu, Daejeon, 305-764, Republic of Korea

[‡]Department of Chemical and Biological Engineering, Tufts University, Medford, Massachusetts 02155, United States

ABSTRACT: Polymeric microparticles with complex shapes have attracted substantial attention in many application areas because particle shape is a critical parameter to impart programmable functionalities. The formation of specific three-dimensional (3D) microstructures in a simple, scalable, and controllable manner is difficult. Here, we report the controlled fabrication of microparticles with complex 3D shapes based on the simple tuning of mold swelling and capillarity. Specifically, a photocurable solution loaded in micromolds is spatially deformed into complex shapes depending on the degree of molding swelling and capillarity, thereby producing polymeric microparticles with controlled 3D shapes upon photopolymerization. The results show that highly uniform microparticles with controlled two-dimensional (2D) and 3D shapes were fabricated from identical 2D micromolds via the simple tuning of the wetting fluids. This technique can be extended to produce highly complex microarchitectures with controlled 3D geometric domains via 2D mold designs. Finally, multicompartment microparticles with independently controlled 3D shapes for each compartment are produced by a simple combination of fabrication sequences. We envision that this strategy of producing 3D microarchitectures from easily designed simple micromolds could provide a path to new materials and new properties.

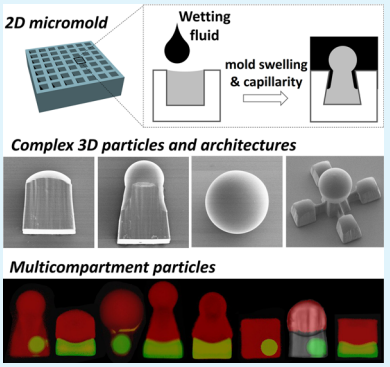

KEYWORDS: *3D geometries, microarchitecture, micromolding, deformation, capillarity*

INTRODUCTION

Polymeric microparticles are important materials used in a number of applications as drug delivery vehicles,[1] tissue engineering scaffolds,[2] building blocks for self-assembly,[3] and multiplexed assays.[4,5] We can control their functionalities by simply tuning their physical properties such as their size, shape, texture, porosity, and compartmentalization.[6,7] Particle shape is a critical parameter that can be readily enlisted to impart programmable functionality.[8,9] For example, nonspherical particles with different surface areas can offer tunable release kinetics for drug delivery applications through the controlled degradation of polymer networks (e.g., zero-order release kinetics from hemispheres).[10,11] In self-assembly applications, particles with controlled three-dimensional (3D) shapes as novel building blocks enable the fabrication of functional superstructures under external stimuli (e.g., magnetic fields). In addition, particles with controlled 3D shapes also enable shape-based encoding for multiplexed high-throughput sensing. Despite the significance of particle shape in these applications, the fabrication of polymeric microparticles with controlled 3D shapes remains challenging because of the lack of simplicity, scalability, and controllability of existing techniques.

Several conventional approaches (e.g., emulsion polymerization, seeded emulsion polymerization, and dispersion polymerization) to fabricate nonspherical polymeric particles (e.g., snowman-like, polyhedral, and disk-shaped particles) have been developed.[12−15] However, these methods involve complicated formulations of chemicals to tune the nucleation and growth and thus do not provide simplicity or high flexibility in controlling the 3D shape. Although particles from conventional bulk approaches can be transformed into nonspherical particles by stretching spherical particles deposited onto polyvinyl films at temperatures greater than the glass-transition temperature (T_g), this technique has limitations with respect to raw materials (e.g., polystyrene or poly(methyl methacrylate)). Microfluidic techniques offer the continuous and rapid fabrication of monodisperse polymeric particles.[16,17] Ellipsoids, rods, and disks have been fabricated by photopolymerization or thermopolymerization of deformed precursor droplets in constricted channel geometries; however, the 3D shapes that can be fabricated using these techniques are limited. Alternatively, flow lithography (FL) techniques have gained substantial attention for the fabrication of monodisperse particles with controlled 3D shapes, for example, stop-flow lithography,[18] lock release lithography,[19] optofluidic maskless lithography,[20] tuning particle curvature using a tuning fluid,[21]

Received: March 4, 2015
Accepted: April 29, 2015
Published: April 29, 2015

DOI: 10.1021/acsami.5b01955
ACS Appl. Mater. Interfaces 2015, 7, 11393−11401

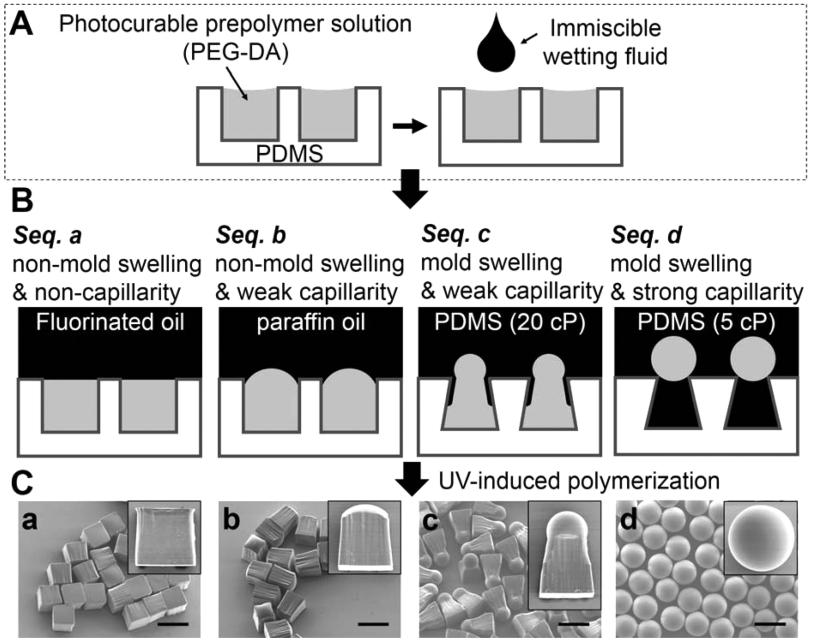

Figure 1. Controlled fabrication of polymeric microparticles with complex 3D shapes by the simple tuning of mold swelling and capillarity. (A) Schematic diagram of the micromolding method with surface-tension-induced flow. (B) Formation of 3D shapes in micromolds, depending on mold swelling and capillarity, upon the addition of four different wetting fluids. (C) SEM images showing the monodisperse polymeric microparticles upon UV-induced polymerization. Scale bars represent 50 μm.

and 3D fluidic self-assembly by axis translation of two-dimensionally fabricated microcomponents.[22] Although these FL techniques offer the ability to rapidly produce particles with controlled shapes, they suffer several inherent drawbacks, including the need for complicated flow control and limited scalability. Multiphoton fabrication techniques have been introduced to expand the capability to produce 3D architectures, but these approaches have limitations for the high-throughput production of microstructures.[23] The DeSimone group has pioneered a micromolding technique called particle replication in a nonwetting template (PRINT).[24] Although the PRINT method can produce monodisperse 2D particles with excellent controllability over a broad range of sizes, the shapes of such particles are limited to predefined mold geometries.

Our approach to addressing these challenges is a simple micromolding method based on surface-tension-induced flow.[25] First, poly(dimethylsiloxane) (PDMS)-based micromolds are filled with photocurable solutions. In the presence of wetting fluids, photopolymerization of the photocurable solutions leads to uniform polymeric microparticles with controlled 3D curvature (i.e., concave or convex) at the top, depending on the surface energy balance.[25] We have shown that this simple method can be readily extended to the production of highly uniform spherical microparticles with controlled size (from a few hundred microns to submicron) and size distribution in a geometrically designed manner.[26] Although these techniques provide simple and robust fabrication of nonspherical 3D particles as well as spherical ones, the fabrication of polymeric microparticles and microarchitectures with controlled 3D shapes with identical molds and compositions remains challenging. In addition, no method to produce both spherical and nonspherical particles with controlled 3D shapes in a simple manner has yet been reported.

In this work, we report the highly controllable fabrication of polymeric microparticles with complex 3D shapes from 2D micromolds based on the simple tuning of capillarity and mold swelling by wetting fluids. Specifically, the simple addition of various wetting fluids allows the spatial deformation of the photocurable solution depending on the degrees of "mold swelling" and "capillarity." Photopolymerization of these deformed solutions leads to highly uniform microparticles with controlled 3D shapes. The results show that this simple tuning of the mold swelling and capillarity allows the fabrication of both nonspherical particles with controlled 3D shapes and spherical particles in an identical mold. The particle shapes can be readily fine-tuned via the simple tuning of the viscosity of the wetting fluids. Moreover, highly complex 3D microarchitectures containing both nonspherical and spherical shapes with controlled multiple geometric domains can also be readily fabricated using simple 2D mold designs. Finally, we demonstrate that multicompartment particles with independently controlled 3D geometries for each compartment can be produced using an identical mold in a sequential manner. Combined, these results illustrate the facile fabrication of complex microparticles with controlled 3D geometries via the simple tuning of mold swelling and capillarity through wetting fluids.

EXPERIMENTAL SECTION

Materials. Poly(ethylene glycol) diacrylate (PEG-DA, M_n = 700), trimethylolpropane triacrylate (TMPTA, M_n = 296), poly(dimethylsiloxane) fluid, Fluorinert FC-40, paraffin oil, *n*-hexadecane, ethanol, isopropyl alcohol, sulforhodamine B, and 2-hydroxy-2-methyl-1-phenyl-propan-1-one (Darocur 1173, photoinitiator) were purchased from Sigma-Aldrich Chemicals (St. Louis, MO). The SU-8 photoresist and developer solution were purchased from MicroChem (Westborough, MA). PDMS (Sylgard 184) was obtained from Dow Corning (Midland, MI).

Fabrication of Micromolds. The micromold was prepared using the conventional soft lithography technique. A mixture of PDMS prepolymer and its curing agent (10:1 ratio) was poured over a silicon

DOI: 10.1021/acsami.5b01955
ACS Appl. Mater. Interfaces 2015, 7, 11393−11401

master and cured at 65 °C. After curing, the PDMS replica was peeled from the silicon master.

Fabrication of polymeric microparticles by UV-induced polymerization: The consistent addition of the PEG-DA in micromolds can be achieved by surface tension force between PEG-DA and PDMS.[25] Wetting fluids are subsequently added and fully covered onto the molds. To fabricate the polymeric microparticles, a photocurable solution (PEG-DA with 1% photoinitiator) in the micromolds was exposed to UV light (100 W HBO mercury lamp) over a wavelength range of 330 to 380 nm (UV-2A filter, Nikon, Japan). The estimated UV exposure time of the droplets in the micromolds was typically less than 30 s. To collect the particles, we gently bend the molds, then the polymerized particles are detached and released away from mold surface without defect of the particles. The particles exposed onto the mold surface can be transferred to a vessel with solvent by directly dipping the molds.

Image Analysis. An inverted fluorescence microscope (TE2000, Nikon, Japan) equipped with a CCD camera (Coolsnap, Photometrics, Tucson, AZ) was used to observe the particle shape and dynamic deformation of the molds. Image analysis of the particles was performed using the ImageJ (National Institute of Health, Maryland) and Image Pro (Media Cybernetics, City, MD) software programs. The detailed morphology of the particles was characterized by scanning electron microscopy (SEM; JEOL, JSM-7000F, Japan) and confocal microscopy (Nikon Eclipse Ti, Japan).

RESULTS AND DISCUSSION

Controlled Fabrication of Complex 3D Microparticles by Simple Tuning Mold Swelling and Capillarity with Identical Molds and Compositions. Here, we report a simple micromolding method to produce polymeric microparticles with highly complex shapes by taking advantage of mold swelling and tunable capillarity, as shown in Figure 1. Specifically, a photocurable solution of PEG-DA was loaded into 2D-shaped micromolds composed of PDMS (Figure 1A). Next, various immiscible wetting fluids were loaded onto the micromold to induce the deformation of the photocurable solution by mold swelling and tunable capillarity (Figure 1B). The deformed solutions were then solidified via UV-induced polymerization, yielding polymeric particles with permanent structures (Figure 1C).

We utilized four types of wetting fluids that confer various degrees of mold swelling and capillarity. The mold swelling occurs when the mold (PDMS) is exposed to the wetting fluid (i.e., a good solvent), and the degree of the mold swelling can be quantified by the swelling coefficient (S) shown in eq 1:[27]

$$S = \frac{D}{D_0} \tag{1}$$

where D is the length of the PDMS in the solvent and D_0 is the length of the dry PDMS. Next, we define capillarity (i.e., capillary penetration) as the ability of a liquid to penetrate into narrow spaces; the liquid's penetrating force can be represented by the Washburn equation (eq 2).[28] The distance l penetrated by a liquid driven by capillary pressure into a capillary tube is given as

$$l = \sqrt{\frac{\gamma r t \cos\theta}{2\mu}} \tag{2}$$

where γ is the liquid surface tension, t is time, r is the radius of the capillary, θ is the contact angle, and μ is the liquid viscosity (see Figures 2 and 3 for further discussion).

First, a fluorinated oil (FC-40, Figure 1B, seq a) provides non-mold swelling and non-capillarity, forming a flat-top interface with the PEG-DA. The fluorinated oil is chemically inert and has negligible solubility with the PDMS mold, leading to non-mold swelling (S = 1.00).[27] Meanwhile, its nonwetting property provides non-capillarity, leading to the flat-top interface. Second, paraffin oil provides non-mold swelling and weak capillarity, forming a convex-top interface (small arrow, Figure 1B, seq b). The paraffin oil also has low solubility with the PDMS mold, leading to nonmold swelling (S = 1.00 ± 0.01).[29] The weak capillarity occurs when the capillary force of the wetting fluid is larger than that of the PEG-DA.[25] The volume of the wetting fluid that moves downward along the PDMS wall leads to an increase in the height of the confined fluid because of mass conservation, thereby forming a convex top to minimize energy.

Next, we used two types of PDMS oil with different viscosities (5 and 20 cP) as good solvents (i.e., the same solubility parameter) to confer significant swelling to the PDMS molds.[27] The schematic of Figure 1B, seq d, shows that the PDMS oil (5 cP) allows mold swelling, whereas its low viscosity leads to strong capillarity, allowing the confined PEG-DA solution to be detached from the bottom surface of the mold. Subsequently, the confined solution becomes a spherical droplet due to energy minimization. The higher viscosity PDMS oil (20 cP) also induces mold swelling, but the wetting fluid does not reach the bottom of the mold because of its low capillary penetration at high fluid viscosity (Figure 1B, seq c).[28] This partial penetration of the oil thus does not lead to the complete detachment of the confined solution or droplet formation. Instead, the deformed PDMS volume given by mold swelling and weak capillarity allows an increase in the height of the confined PEG-DA and forms the convex-top interface (Figure 1B, seq c).

Figure 1C shows SEM images of the complex microparticles fabricated under four wetting-fluid conditions from identical square-shaped PDMS molds. First, Figure 1C-a shows that uniform flat-top cuboid particles (2D shape) were formed by non-mold swelling and non-capillarity (seq a), whereas Figure 1C-b shows convex-top particles from the non-mold swelling and weak capillarity condition (seq b). Figure 1C-c shows that mold swelling and weak capillarity (seq c) leads to complex 3D particles with both spherical and nonspherical domains. We noted that the relatively smooth edges (compared to the faces of the particles) of the particles in the SEM images implies that the wetting fluid (PDMS 20 cP) penetrated through the edges of the mold. Finally, Figure 1C-d shows highly monodisperse (coefficient of variation (CV) = 2.5%) and entirely spherical particles from mold swelling and strong capillarity (seq d), consistent with our recent results.[30]

The SEM images in Figure 1C show several features of our micromolding method. First, all of the particles formed are consistently uniform under all of the four different wetting-fluid conditions. Second, this micromolding method leads to the production of complex particles with near 100% fidelity, as partially represented by the low CV value for the spherical particles (Figure 1C-d). Third, this robust technique enables a delicate balance between mold swelling and capillarity to be readily achieved via the simple tuning of the wetting fluids (Figure 1C-c). Finally, this method leads to various 2D- and 3D-shaped particles with identical volumes from identical mold geometries and dimensions. This feature suggests that the technique can be further extended to the production of complex particles with various compositions through other solidification schemes (e.g., sol−gel reactions).[30]

DOI: 10.1021/acsami.5b01955
ACS Appl. Mater. Interfaces 2015, 7, 11393−11401

Compared to microfluidic techniques, our micromolding method presents several advantages in the fabrication of complex microparticles, as indicated by the results in Figure 1. First, the procedure allows for the production of highly uniform polymeric particles without the need for delicate flow control, unlike microfluidic approaches. Second, this technique provides precise control of the particle shape by simply utilizing different wetting fluids in an identical manner. Third, further flexibility in particle shape control was readily achieved by enlisting other 2D mold geometries (Figure 3). Finally, this technique does not require the use of surfactants to form monodisperse spherical particles because the droplets are physically isolated and stabilized inside each micromold during the UV-induced polymerization.

Due to the simplicity and robustness of our technique, we envision the fabrication of complex multidomain particles consisting of discrete domains in terms of chemistry, functionality, or both. For example, nanoparticles with two different sizes could be mixed with a photocurable solution, where each type of nanoparticle could then be spontaneously incorporated near the top or bottom regions of the particles depending on their specific gravity, thereby leading to Janus particles with two distinct functionalities. In addition, particles with controlled shapes could be potentially useful in drug delivery applications, where the shape could be enlisted as an important design parameter to impart desired cellular internalization and vascular dynamics.[31] In summary, the results in Figure 1 demonstrate that our simple micromolding technique enables the production of highly complex and uniform polymeric microparticles via the simple tuning of mold swelling, capillarity, or both.

Quantitative Analysis of Varying Particle Shapes on Tunable Mold Swelling and Capillarity. We next examined how the particle morphology could be tuned by the mold swelling and/or the capillarity, as shown in Figure 2. For these experiments, PDMS micromolds containing identical volumes of PEG-DA as the photocurable solution under three wetting-fluid conditions (top view) were examined over a period of 500 s via sequential micrographs, and the resulting microparticle morphologies with various mold swelling times upon UV exposure were also examined (side view).

First, Figure 2A shows that the non-swelling and weak capillarity condition (seq b) allows negligible mold swelling (top view), whereas the resulting particles exposed to the wetting fluid for various times show the rapid formation of a convex top within the first 20 s (side view). Figure 2B shows that the swelling and weak capillarity condition (seq c) leads to moderate mold swelling, as indicated by the reduction of the area of the mold to approximately 57% of the original dimensions (top view). Next, the side views of the resulting particles show the evolution of the 3D morphologies over time. We observed the similar convex top formation within 20 s. Then, as the mold continues to swell, the compressed volume of the swollen mold leads to the increased height of the resulting particle over time. Finally, Figure 2C shows that the swelling and strong capillarity condition (seq d) leads to significant mold swelling, as indicated by the reduction of the area of the mold to approximately 33% (top view). The strong capillarity of the wetting fluid leads to deeper penetration along the side wall of the mold, increasing the exposure of the molds to the wetting fluid for further compression of the mold volume. As the wetting fluid reaches the bottom surface, the PEG-DA detaches from the bottom, thereby forming spherical

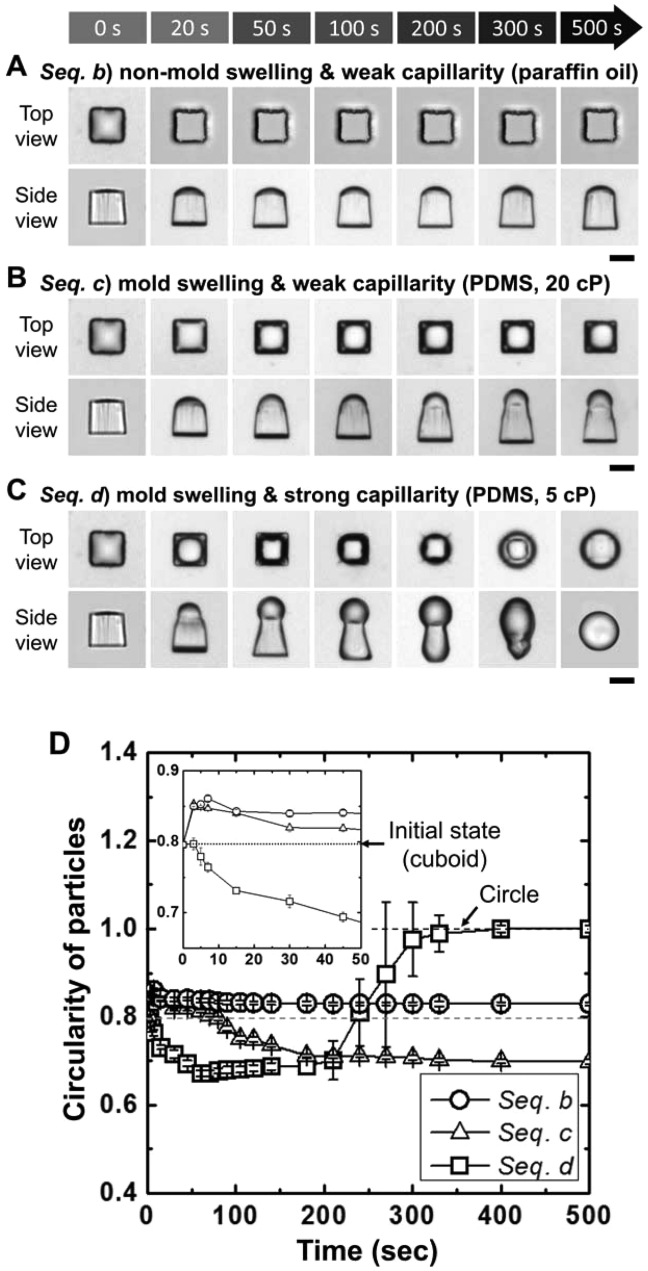

Figure 2. Quantitative analysis of various particle shapes induced by tunable mold swelling and capillarity. (A–C) Sequential micrographs showing the deformation of the micromolds (top view) and the resulting particles (side view) with various exposure times to different wetting fluids; (A) paraffin oil, (B) PDMS (20 cP), and (C) PDMS (5 cP). (D) Plot showing the evolution of particle shapes (represented by circularity) with various exposure times to the wetting fluids. Scale bars represent 50 μm.

particles. Because the non-swelling and non-capillarity (seq a) does not vary with the exposure time to the wetting fluid, the data are not presented. Meanwhile, the non-swelling and weak capillarity condition (seq b) shown in Figure 1B, seq b, does not show the evolution of the morphology over the time period examined (data not shown).

Next, we express the dynamic deformation of the PEG particles (Figure 2A–C) in terms of "circularity"[32] as shown in Figure 2D. Here, the circularity is defined as

DOI: 10.1021/acsami.5b01955
ACS Appl. Mater. Interfaces 2015, 7, 11393–11401

$$\text{circularity} = \frac{4\pi A}{P^2} \quad (3)$$

where A is the projected area of the particles in the side view (Figure 2A−C), and P is their perimeter. The circularity ranges from 0 (elongated polygon) to 1 (perfect circle); that is, particles with more complex geometries (e.g., the particles in Figure 2B) will exhibit low circularity values.

First, the non-swelling and weak capillarity condition (Figure 2A,D, ○) shows a minimal change in the circularity over time. Second, the swelling and weak capillarity condition (Figure 2B,D, △) shows a slow change in the circularity that reaches an equilibrium state after 200 s. An enlarged plot Figure 2E shows the early stage of the circularity evolution over 50 s, indicating similar trends of increasing circularity over the first 10 s under these two conditions (○ and △). This result implies that the initial increase in the circularity originates from the capillarity of the wetting fluids, whereas the subsequent decrease in the circularity results from the mold swelling. Thus, this difference in the time-dependent evolution between the two conditions (i.e., nonswelling vs swelling, A vs B) indicates that the mold swelling plays a key role in tuning the particle geometry. Next, the swelling and strong capillarity condition (Figure 2C,D, □) shows two transition states: the circularity rapidly decreases for the first 50 s and then starts increasing substantially after 200 s, reaching equilibrium by 400 s. This result indicates that the rapid decrease of the circularity in the first transition state (~50 s) is due primarily to the spatial deformation of the PEG-DA by rapid mold swelling and capillarity, whereas the second transition originates from the evolution of the PEG-DA to spherical droplets by surface-tension-induced flow in the z-direction (i.e., Laplace pressure-driven flow). Notably, the consistently small error bars from 100 particles collected for each condition over time indicates the reliable and consistent evolution of morphologies, whereas the large error bars in the swelling & strong capillarity condition within the 200−300 s time frame represents variability in the abrupt transition to spherical droplets.

We further illustrate that our simple method can be readily extended to further fine-tune the particle shape via simple tuning of the viscosity of the wetting fluids (Figure 3). In these experiments, we varied the viscosity of the wetting fluids from 5 to 50 cP by simply mixing two PDMS oils with different viscosities. All the wetting fluids used here have identical surface tensions and wettabilities on PDMS substrates (22 mN/m and complete wetting). The surface tension values imply that the viscosity of the wetting fluids is a key factor for tuning the capillarity (eq 2). The particles were prepared by polymerizing the PEG-DA after it had reached an equilibrium state (500 s). Figure 3A shows a plot of the circularity of the resulting particles as a function of the viscosities of the wetting fluids. Low-viscosity wetting fluids (<10 cP) led to the formation of spherical particles, whereas higher-viscosity wetting fluids (>18 cP) led to nonspherical particles. Importantly, the circularity of the particles prepared using higher-viscosity wetting fluids could be precisely tuned (0.7−0.8) by simply varying the viscosity (i.e., mixing two wetting fluids, 17−50 cP) in a consistent manner, as evidenced by the small error bars. This result in Figure 3A indicates that the viscosity of the wetting fluids is a useful fabrication parameter for tuning the penetration length (L) on the basis of Washburn equation, thereby enabling further control of the particle morphologies. This precise control of the penetration length (and thus particle morphology) is further illustrated in Figure 3B, where the measured penetration lengths correlate well with the viscosity of the wetting fluids. Specifically, wetting fluids with viscosities from 17 to 50 cP led to penetration lengths of 62 to 14 μm in a consistent manner (i.e., small error bars from 100 particles for each condition).

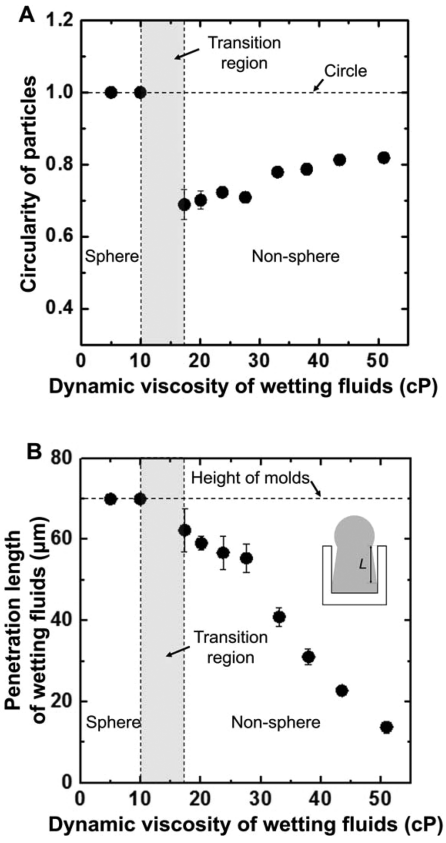

Figure 3. Fine-tuning the particle shape by varying the dynamic viscosity of the wetting fluids. Plots show (A) the circularity of the resulting particles and (B) the estimated penetration lengths (L) resulting from variation of the viscosity of the wetting fluid (PDMS oil); the circularity ranges from 0 (elongated polygon) to 1 (perfect circle).

The results in Figures 2 and 3 indicate that the particle shape was precisely controlled by capturing the dynamic deformation of the PEG-DA via the simple UV-induced polymerization as well as by simply tuning the viscosity of the wetting fluids. In summary, the in-depth analysis and quantification results in Figures 2 and 3 corroborate the controlled fabrication of microparticles with complex 3D shapes shown in Figure 1 and provide simple design parameters for further fine-tuning and control (e.g., dynamic evolution and viscosity).

Fabrication of Complex Microarchitectures with Controlled 3D Domains by Simple 2D Mold Designs. The ability to tune the mold swelling and capillarity can be extended to the fabrication of highly complex 3D microarchitectures via simple 2D geometric mold design. To examine this application, we used mold designs consisting of different-sized squares connected with branches (Figure 4). As shown in the schematic diagram of Figure 4A, the addition of wetting fluids (PDMS oil with 20 cP for swelling and weak capillarity, seq c) into the micromold containing the PEG-DA led to convex top formation with a different radius of curvature in each square region (Figure 4A-a,b). This difference in the

DOI: 10.1021/acsami.5b01955
ACS Appl. Mater. Interfaces 2015, 7, 11393−11401

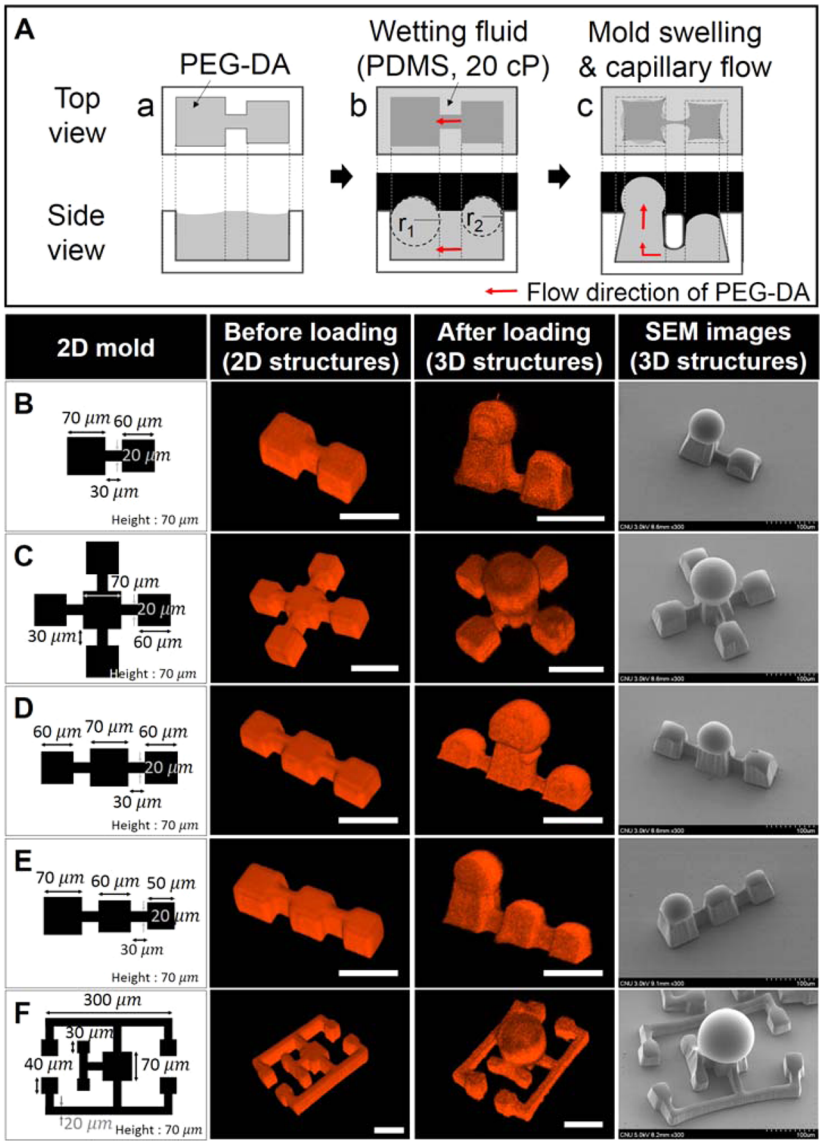

Figure 4. Complex microarchitectures with 3D domains controlled by simple 2D mold designs. (A) Schematic showing the mechanism of formation of the PEG-DA solution by surface-tension-induced flow. Various 2D mold designs (first column) consisting of (B–D) two different-sized squares and (E) three different-sized squares, and (F) a complex microchannel. Confocal microscopy images (second and third columns) showing the formation of the PEG-DA solution with and without the addition of wetting fluids. SEM images (fourth column) showing the formation of the resulting particles upon UV-induced polymerization. Scale bars represent 100 μm.

radius of curvature causes the PEG-DA to flow (denoted as arrow) into the larger square region (quantifiable by the Laplace pressure).[33] Figure 4A-c shows that that the swelling and weak capillarity condition (seq c) induces compression of the mold, further increasing the flow of the PEG-DA. This Laplace pressure-driven flow of the PEG-DA leads to the formation of asymmetric 3D microarchitectures. Figure 4B–F show that this principle, combined with simple 2D mold designs, enables the fabrication of a wide range of complex 3D microarchitectures. The evolutions of the PEG-DA (mixed with sulforhodamine B) before and after the addition of the wetting fluid were examined via confocal microscopy (z-stack images, two middle columns), and the resulting particles were further characterized by SEM.

The first column of Figure 4B–F shows the various 2D mold designs, consisting of two different-sized squares (Figures 4B-D), three different-sized squares (Figure 4E), and a complex microchannel (Figure 4F) to impart directional flows. The confocal images in the second column of Figure 4B–F show that the PEG-DA is uniformly loaded into each mold before the addition of wetting fluids, representing the original mold geometries and dimensions. The confocal images in the third column of Figure 4B–F show the completed evolutions of the PEG-DA after addition of the wetting fluids. These results indicate that simple 2D mold designs guide the flow of the PEG-DA (through the branches) to the desired regions, leading to convex-top formation in the larger square region. The SEM images in the fourth column of Figures 4B–F show that highly complex 3D microarchitectures can be readily fabricated by the UV-induced polymerization of the PEG-DA. Specifically, mold designs consisting of two different-sized squares lead to convex-top formation on the larger square region (Figure 4B–D) with greater curvature than in the single 2D domain designs shown in Figure 2. A mold design consisting of three different-sized squares provides a differential pressure gradient among them, leading to the formation of hierarchical structures with different

DOI: 10.1021/acsami.5b01955
ACS Appl. Mater. Interfaces 2015, 7, 11393–11401

heights and curvatures in each region (Figure 4E). Finally, more complex channel geometries with a larger PEG-DA supply volume, as shown in Figure 4F, can lead to the formation of a more complete spherical region.

Although microfluidic and micromolding techniques can produce either spherical or nonspherical shapes,[18,24,25,30] the controlled fabrication of complex microarchitectures possessing both shapes remains highly challenging. To the best of our knowledge, the results shown in Figure 4 are the first demonstration of the fabrication of complex 3D microparticles with both spherical and nonspherical shapes in a single particle. We envision that this simple technique can be readily extended to produce functional materials. For example, microparticles incorporating magnetic colloids could be used for microturbines with high performance for mixing.[34] Specifically, the spherical part can allow for rapid rotation with negligible friction, and the nonspherical part can allow for chaotic flow to provide efficient mixing. Combined, the results in Figure 4 indicate that polymeric particles with highly complex 3D geometries can be readily fabricated using simple 2D mold designs.

Fabrication of Multicompartment Microparticles with Independently Controlled 3D Shapes for Each Compartment. Finally, we demonstrate that our simple micromolding technique can be readily extended to produce various multicompartment microparticles with controlled 3D shapes in a sequential manner, as shown in Figure 5. Specifically, the schematic diagram of Figure 5A shows that a primary compartment (1) is first introduced into the micromolds by the addition of the PEG-DA in a volatile solvent (i.e., ethanol) and subsequent solvent evaporation. Depending on the presence or absence of the wetting fluid (PDMS oil, 20 cP), the shape of this primary compartment can be controlled to be concave (Route 1, top row) or spherical (Route 2, second row) on the basis of the surface energy balance.[25] Upon UV-induced polymerization of this primary compartment, the secondary compartment (2) is fabricated by simply repeating the aforementioned procedure, where various wetting fluids can be used to confer further 3D shapes (second process), as shown in Figure 1B. To visualize each compartment, we incorporated fluorescein (green) in the primary compartments and sulforhodamine B (red) in the secondary ones by mixing them with the PEG-DA solution.

The schematics and corresponding bright-field-fluorescence composite micrographs shown in Figure 5 indicate that multicompartment microparticles with nonsphere/nonsphere and sphere/nonsphere configurations were fabricated by combining sequences (seqs a–d shown in Figure 1B) via Routes 1 (left column) and 2 (right column), respectively. First, Figure 5B shows that Route 1 leads to concave-flat microparticles by combining seq a (FC oil), whereas concave-convex ones are fabricated by combining seq b (paraffin oil) (Figure 5C). As shown in Figure 5D,E, further flexibility to control the shapes of the particles was achieved by combining seqs c and d using wetting fluids with different viscosities (PDMS oils with 20 cP and 5 cP). In addition, bicompartment spherical/nonspherical microparticles can also be fabricated via Route 2 (right column of Figure 5). Figures 5F–H show that the microspheres fabricated as the primary compartment are consistently enclosed in cuboid, bullet-like, and larger spherical particles as the secondary compartment, whose shapes are controlled by combining seq a (FC-40), seq c (PDMS oil, 20 cP), and seq d (PDMS oil, 5 cP). Finally, Figure 5I shows that

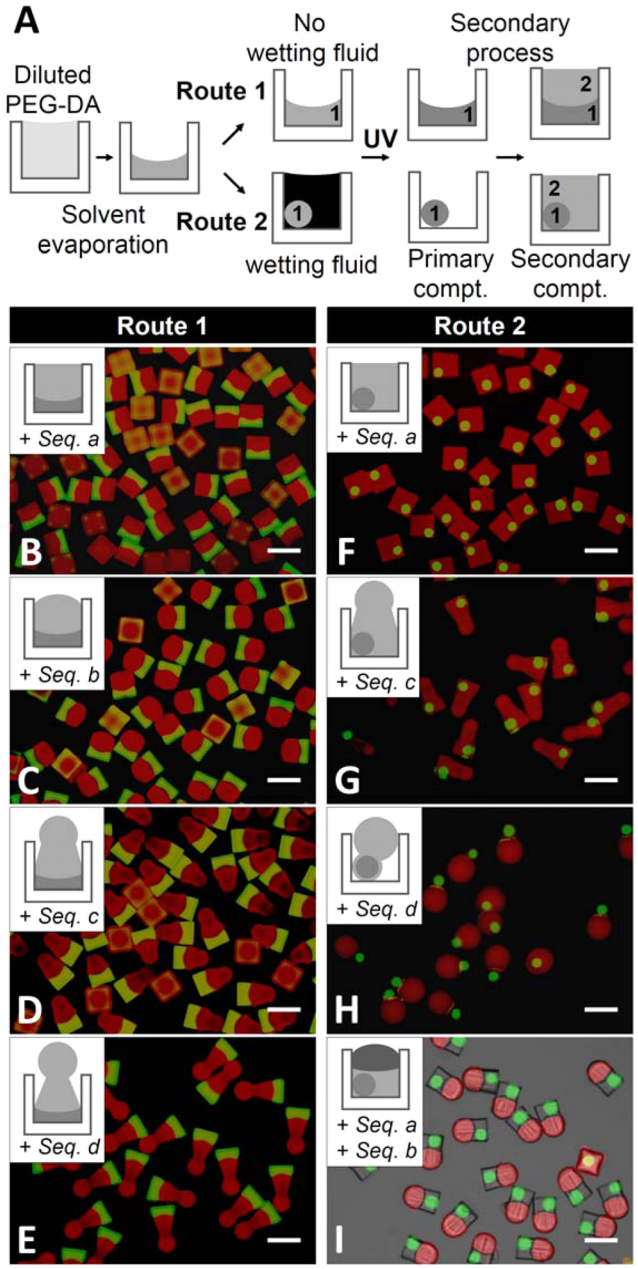

Figure 5. Multicompartment microparticles with independently controlled 3D shapes for each compartment. (A) Schematic showing the sequential micromolding procedure used to produce multicompartment microparticles with nonsphere/nonsphere and sphere/nonsphere formation via routes 1 and 2, respectively. "Compartment" is abbreviated as "compt." (B–I) Schematics (insets) and corresponding composite micrographs of the multicompartment microparticles prepared by combining sequences (seqs a–d, shown in Figure 1B); nonsphere/nonsphere particles with (B) concave-flat and (C-E) concave-convex shapes, and sphere/nonsphere particles with (F) cuboid, (G) bullet-like, and (H) snowman-like shapes. (I) Tricompartment particles possessing spherical, concave, and convex shapes prepared by combining multiple sequences. Scale bars represent 100 μm.

tricompartment microparticles possessing spherical, concave, and convex shapes within a single particle can be fabricated by combining multiple sequences (seqs a and b).

The fabrication of multicompartment microparticles (i.e., cylinders, dumbbell-like, and core–shell spherical particles) has

DOI: 10.1021/acsami.5b01955
ACS Appl. Mater. Interfaces 2015, 7, 11393–11401

been demonstrated by sequential micromolding methods;[25,35,36] however, controlling the 3D shapes remains a challenge. The results shown in Figure 5 illustrate that our micromolding technique enables the fabrication of multicompartment microparticles with independently controlled 3D shapes for each compartment in a sequential manner. In addition, the uniformity and consistency of the microparticles are well-maintained, further indicating the robustness of our wetting-fluid-based strategy in the sequential procedure employed here. Importantly, the flexible nature of our simple wetting-fluid-based shape control negates the need for delicate control of multiphasic flows or balancing the surface energy between each phase, unlike continuous microfluidic approaches.

The sequential fabrication of multicompartment microparticles with controlled 3D shapes shown in Figure 5 could be utilized to manufacture multifunctional particles with discrete functionalities in each compartment within a single particle. For example, anisotropic incorporation of magnetic nanoparticles into the primary compartment could provide a magnetic functionality with programmable loading for separation[37] or self-assembly into 3D superstructures.[38] Additionally, such multicompartment particles could be utilized for the simultaneous encapsulation of multiple cargos within a single particle[39] so that their release profiles could be controlled via tuning of particle shapes and surface areas. In addition, the ability to tune 3D shapes and the number of compartments could also provide alternative routes to shape-based encoding systems for multiplexed sensing.[40] Combined, the results shown in Figure 5 indicate that our micromolding technique can be enlisted in a simple sequential manner to fabricate multicompartment particles with independently controlled 3D shapes for each compartment using identical molds in a consistent manner.

CONCLUSIONS

In this study, we have demonstrated the controlled fabrication of polymeric microparticles with complex 3D shapes based on the simple tuning of the capillarity and mold swelling by wetting fluids. Polymeric microparticles with various 3D shapes were consistently fabricated by the simple addition of various wetting fluids depending on the degree of mold swelling and capillarity. Highly complex microarchitectures possessing both nonspherical and spherical shapes with controlled geometrical domains were also fabricated by simple 2D mold designs. Finally, we demonstrated that multicompartment microparticles with independently controlled 3D shapes for each compartment could also be readily fabricated in a sequential manner. Taken together, these results illustrate the general and specific advantages of our batch-processing-based micromolding technique and wetting-fluid-based shape control. First, this technique provides for the precise control of the particle shape by simply utilizing various wetting fluids in an identical platform. Second, the fabrication of uniform and complex microparticles can be achieved without the use of surfactants because the precursor solutions (e.g., deformed solution or spherical droplets) are physically stabilized inside each micromold. Thus, this technique can be considered as a green fabrication process. Third, this technique allows for the fabrication of complex microparticles in a cost-efficient manner, without the need for expensive apparatus and delicate hydrodynamic control, unlike microfluidic techniques. Fourth, our method can be readily scaled for mass production through parallelization. Furthermore, this technique can be adapted to fabricate substantially smaller complex particles (i.e., submicrometer scale) by simply controlling the confined volume of the prepolymer via solvent evaporation.[26] We envision our technique for the controlled fabrication of microparticles with complex 3D shapes being readily extended to produce a wide range of materials with controlled functionalities, such as drug delivery vehicles for controlled release, shape-based encoded particles for multiplexed assays, and novel building blocks for self-assembly.

AUTHOR INFORMATION

Corresponding Author

*E-mail: rhadum@cnu.ac.kr.

Present Address

[§]School of Engineering and Applied Sciences, Department of Physics, Harvard University, Cambridge, MA 02138, United States

Author Contributions

[∥]These authors contributed equally.

Notes

The authors declare no competing financial interest.

ACKNOWLEDGMENTS

We acknowledge financial support from the Basic Science Research Program through the National Research Foundation of Korea (NRF) funded by the Ministry of Science, ICT & Future Planning (MSIP) (No. NRF-2011-0017322) and by the Space Core Technology Program through the National Research Foundation of Korea (NRF) funded by the Ministry of Science, ICT & Future Planning (NRF-2013M1A3A3A02042262).

REFERENCES

(1) LaVan, D. A.; McGuire, T.; Langer, R. Small-Scale Systems for in Vivo Drug Delivery. *Nat. Biotechnol.* **2003**, *21*, 1184−1191.

(2) Khademhosseini, A.; Langer, R. Microengineered Hydrogels for Tissue Engineering. *Biomaterials* **2007**, *28*, 5087−5092.

(3) Dendukuri, D.; Doyle, P. S. The Synthesis and Assembly of Polymeric Microparticles Using Microfluidics. *Adv. Mater.* **2009**, *21*, 4071−4086.

(4) Pregibon, D. C.; Toner, M.; Doyle, P. S. Multifunctional Encoded Particles for High-Throughput Biomolecule Analysis. *Science* **2007**, *315*, 1393−1396.

(5) Eun Chung, S.; Kim, J.; Yoon, O. D.; Song, Y.; Hoon Lee, S.; Min, S.; Kwon, S. One-Step Pipetting and Assembly of Encoded Chemical-laden Microparticles for High-Throughput Multiplexed Bioassays. *Nat. Commun.* **2014**, *5*, 3468−3479.

(6) Mitragotri, S.; Lahann, J. Physical Approaches to Biomaterial Design. *Nat. Mater.* **2009**, *8*, 15−23.

(7) Choi, C. H.; Weitz, D. A.; Lee, C. S. One-Step Formation of Controllable Complex Emulsions: From Functional Particles to Simultaneous Encapsulation of Hydrophilic and Hydrophobic Agents into Desired Position. *Adv. Mater.* **2013**, *25*, 2536−2541.

(8) Champion, J. A.; Katare, Y. K.; Mitragotri, S. Particle Shape: A New Design Parameter for Micro- and Nanoscale Drug Delivery Carriers. *J. Controlled Release* **2007**, *121*, 3−9.

(9) Park, J. Y. Lithographically Patterned Micro-/Nanostructures via Colloidal Lithography. *Korean J. Chem. Eng.* **2014**, *31*, 541−547.

(10) Hsieh, D. S. T.; Rhine, W. D.; Langer, R. Zero-Order Controlled-Release Polymer Matrices for Micromolecules and Macromolecules. *J. Pharm. Sci.* **1983**, *72*, 17−22.

(11) Devi, M. G.; Dutta, S.; Al Hinai, A. T.; Feroz, S. Studies on Encapsulation of Rifampicin and Its Release from Chitosan-Dextran Sulfate Capsules. *Korean J. Chem. Eng.* **2014**, *32*, 118−124.

DOI: 10.1021/acsami.5b01955
ACS Appl. Mater. Interfaces 2015, 7, 11393−11401

(12) Fujibayashi, T.; Okubo, M. Preparation and Thermodynamic Stability of Micron-sized, Monodisperse Composite Polymer Particles of Disc-like Shapes by Seeded Dispersion Polymerization. *Langmuir* **2007**, *23*, 7958−7962.
(13) Tanaka, T.; Komatsu, Y.; Fujibayashi, T.; Minami, H.; Okubo, M. A Novel Approach for Preparation of Micrometer-sized, Monodisperse Dimple and Hemispherical Polystyrene Particles. *Langmuir* **2010**, *26*, 3848−3853.
(14) Kim, J. W.; Larsen, R. J.; Weitz, D. A. Synthesis of Nonspherical Colloidal Particles with Anisotropic Properties. *J. Am. Chem. Soc.* **2006**, *128*, 14374−14377.
(15) Hwang, K.; Ha, K. Synthesis and Characterization of Cross-linked Poly(acrylic acid)−Poly(styrene-alt-maleic anhydride) Core−Shell Microcapsule Absorbents for Cement Mortar. *Korean J. Chem. Eng.* **2014**, *31*, 911−917.
(16) Xu, S. Q.; Nie, Z. H.; Seo, M.; Lewis, P.; Kumacheva, E.; Stone, H. A.; Garstecki, P.; Weibel, D. B.; Gitlin, I.; Whitesides, G. M. Generation of Monodisperse Particles by Using Microfluidics: Control over Size, Shape, and Composition. *Angew. Chem., Int. Ed.* **2005**, *44*, 724−728.
(17) Dendukuri, D.; Tsoi, K.; Hatton, T. A.; Doyle, P. S. Controlled Synthesis of Nonspherical Microparticles Using Microfluidics. *Langmuir* **2005**, *21*, 2113−2116.
(18) Dendukuri, D.; Gu, S. S.; Pregibon, D. C.; Hatton, T. A.; Doyle, P. S. Stop-Flow Lithography in a Microfluidic Device. *Lab Chip* **2007**, *7*, 818−828.
(19) Bong, K. W.; Pregibon, D. C.; Doyle, P. S. Lock Release Lithography for 3D and Composite Microparticles. *Lab Chip* **2009**, *9*, 863−866.
(20) Chung, S. E.; Park, W.; Shin, S.; Lee, S. A.; Kwon, S. Guided and Fluidic Self-Assembly of Microstructures Using Railed Microfluidic Channels. *Nat. Mater.* **2008**, *7*, 581−587.
(21) Panda, P.; Yuet, K. P.; Hatton, T. A.; Doyle, P. S. Tuning Curvature in Flow Lithography: A New Class of Concave/Convex Particles. *Langmuir* **2009**, *25*, 5986−5992.
(22) Chung, S. E.; Jung, Y.; Kwon, S. Three-Dimensional Fluidic Self-Assembly by Axis Translation of Two-Dimensionally Fabricated Microcomponents in Railed Microfluidics. *Small* **2011**, *7*, 796−803.
(23) LaFratta, C. N.; Fourkas, J. T.; Baldacchini, T.; Farrer, R. A. Multiphoton Fabrication. *Angew. Chem., Int. Ed.* **2007**, *46*, 6238−6258.
(24) Rolland, J. P.; Maynor, B. W.; Euliss, L. E.; Exner, A. E.; Denison, G. M.; DeSimone, J. M. Direct Fabrication and Harvesting of Monodisperse, Shape-Specific Nanobiomaterials. *J. Am. Chem. Soc.* **2005**, *127*, 10096−10100.
(25) Choi, C. H.; Lee, J.; Yoon, K.; Tripathi, A.; Stone, H. A.; Weitz, D. A.; Lee, C. S. Surface-Tension-Induced Synthesis of Complex Particles Using Confined Polymeric Fluids. *Angew. Chem., Int. Ed.* **2010**, *49*, 7748−7752.
(26) Choi, C. H.; Kim, J.; Kang, S. M.; Lee, J.; Lee, C. S. Controllable Preparation of Monodisperse Microspheres Using Geometrically Mediated Droplet Formation in a Single Mold. *Langmuir* **2013**, *29*, 8447−8451.
(27) Lee, J. N.; Park, C.; Whitesides, G. M. Solvent Compatibility of Poly(dimethylsiloxane)-based Microfluidic Devices. *Anal. Chem.* **2003**, *75*, 6544−6554.
(28) Washburn, E. W. The Dynamics of Capillary Flow. *Phys. Rev.* **1921**, *17*, 273−283.
(29) Dangla, R.; Gallaire, F.; Baroud, C. N. Microchannel Deformations Due to Solvent-Induced PDMS Swelling. *Lab Chip* **2010**, *10*, 2972−2978.
(30) Choi, C. H.; Jeong, J. M.; Kang, S. M.; Lee, C. S.; Lee, J. Synthesis of Monodispersed Microspheres from Laplace Pressure Induced Droplets in Micromolds. *Adv. Mater.* **2012**, *24*, 5078−5082.
(31) Champion, J. A.; Mitragotri, S. Role of Target Geometry in Phagocytosis. *Proc. Natl. Acad. Sci. U.S.A.* **2006**, *103*, 4930−4934.
(32) Komabayashi, T.; Spangberg, L. S. W. Comparative Analysis of the Particle Size and Shape of Commercially Available Mineral Trioxide Aggregates and Portland Cement: A Study with a Flow Particle Image Analyzer. *J. Endodont.* **2008**, *34*, 94−98.
(33) Walker, G. M.; Beebe, D. J. A Passive Pumping Method for Microfluidic Devices. *Lab Chip* **2002**, *2*, 131−134.
(34) Tian, Y.; Zhang, Y. L.; Ku, J. F.; He, Y.; Xu, B. B.; Chen, Q. D.; Xia, H.; Sun, H. B. High Performance Magnetically Controllable Microturbines. *Lab Chip* **2010**, *10*, 2902−2905.
(35) Choi, C. H.; Kang, S. M.; Jin, S. H.; Yi, H.; Lee, C. S. Controlled Fabrication of Multi-compartmental Polymeric Microparticles by Sequential Micromolding via Surface-Tension-Induced Droplet Formation. *Langmuir* **2014**, 1328−1335.
(36) Kang, S. M.; Kumar, A.; Choi, C. H.; Tettey, K. E.; Lee, C. S.; Lee, D.; Park, B. J. Triblock Cylinders at Fluid−Fluid Interfaces. *Langmuir* **2014**, *30*, 13199−13204.
(37) Shah, R. K.; Kim, J. W.; Weitz, D. A. Janus Supraparticles by Induced Phase Separation of Nanoparticles in Droplets. *Adv. Mater.* **2009**, *21*, 1949−1953.
(38) Yan, J.; Bloom, M.; Bae, S. C.; Luijten, E.; Granick, S. Linking Synchronization to Self-Assembly Using Magnetic Janus Colloids. *Nature* **2012**, *491*, 578−581.
(39) Hu, S. H.; Chen, S. Y.; Gao, X. H. Multifunctional Nanocapsules for Simultaneous Encapsulation of Hydrophilic and Hydrophobic Compounds and On-Demand Release. *ACS Nano* **2012**, *6*, 2558−2565.
(40) Lewis, C. L.; Choi, C. H.; Lin, Y.; Lee, C. S.; Yi, H. Fabrication of Uniform DNA-Conjugated Hydrogel Microparticles via Replica Molding for Facile Nucleic Acid Hybridization Assays. *Anal. Chem.* **2010**, *82*, 5851−5858.

DOI: 10.1021/acsami.5b01955
ACS Appl. Mater. Interfaces 2015, 7, 11393−11401